

QKI dysregulation induces extensive splicing changes in T-cell acute lymphoblastic leukemia

Bruno Palhais,^{1-4*} Nitesh D. Sharma,^{5,6*} Igor Fijalkowski,^{1,2,4} Tim Pieters,^{1-4,7} Dieter Deforce,^{2,8,9} Filip Van Nieuwerburgh,^{2,8,9} Pieter Mestdagh,^{1,2,10#} Panagiotis Ntziachristos,^{1,2,4#} Ksenia Matlawska-Wasowska^{5,6#} and Pieter Van Vlierberghe^{1-3#†}

¹Center for Medical Genetics, Ghent University and University Hospital, Ghent, Belgium;

²Cancer Research Institute Ghent (CRIG), Ghent, Belgium; ³Normal and Malignant

Hematopoiesis Lab, Department of Biomolecular Medicine, Ghent University, Ghent, Belgium;

⁴Leukemia Therapy Resistance Unit, Department of Biomolecular Medicine, Ghent University,

Ghent, Belgium; ⁵Department of Cell, Developmental and Integrative Biology, University of

Alabama at Birmingham, Birmingham, AL, USA; ⁶Department of Pediatrics, University of New

Mexico, Albuquerque, NM, USA; ⁷Unit for Translational Research in Oncology, Department of

Diagnostic Sciences, Ghent University, Ghent, Belgium; ⁸Laboratory of Pharmaceutical

Biotechnology, Department of Pharmaceutics, Ghent University, Ghent, Belgium; ⁹NXTGNT,

Ghent University, Ghent, Belgium and ¹⁰OncoRNALab, Department of Biomolecular Medicine,

Ghent University, Ghent, Belgium

* *BP and NDS contributed equally as first authors.*

PM, PN, KM-W and PVV contributed equally as senior authors.

† *Deceased.*

Correspondence: K. Matlawska-Wasowska
kmatlawska@uab.edu

P. Ntziachristos
panagiotis.ntziachristos@ugent.be

P. Mestdagh
pieter.mestdagh@ugent.be


B. Palhais
bruno.palhais@ugent.be

Received: March 25, 2025.

Accepted: December 30, 2025.

Early view: January 15, 2026.

<https://doi.org/10.3324/haematol.2025.287809>

Published under a CC BY license 

Abstract

Understanding the molecular mechanisms underlying T-cell acute lymphoblastic leukemia (T-ALL) is essential for developing more effective therapeutic strategies. Despite therapeutic advances, the role of RNA-binding proteins in the pathogenesis of T-ALL remains poorly understood. Here, we investigate the RNA-binding Quaking protein (QKI), identifying it as a key regulator of splicing with tumor-suppressive properties in T-ALL. Through the analysis of two independent pediatric T-ALL cohorts, we demonstrate that *QKI* expression is frequently reduced in T-ALL, particularly within the HOXA subtype, and this reduction correlates with poor overall and event-free survival. Using T-ALL cell lines, we show that QKI depletion induces widespread splicing alterations, with numerous events corroborated in patient samples. Transcriptome profiling indicates that *QKI* downregulation leads to broad changes in gene expression, notably affecting pathways related to cell cycle progression, cholesterol homeostasis, and epithelial-mesenchymal transition. Functional assays demonstrate that *QKI* overexpression in T-ALL cells significantly reduces cell proliferation, induces G0/G1 cell cycle arrest, and limits leukemia progression and dissemination, ultimately improving survival in xenograft models. Together, these findings provide compelling evidence that *QKI* functions as a regulator of RNA splicing with tumor-suppressive activity in T-ALL.

Introduction

T-cell acute lymphoblastic leukemia (T-ALL) is an aggressive hematologic malignancy originating from the malignant transformation of T-cell precursors. Accounting for approximately 15% of pediatric and 25% of adult acute lymphoblastic leukemia (ALL) cases, T-ALL is characterized by a high degree of genetic and molecular heterogeneity.^{1,2} T-ALL patients can be classified into different molecular subgroups based on transcriptome profiles and genomic alterations of specific oncogenic transcription factors, such as TAL1, TLX1, TLX3, HOXA9/10, LMO2 or NKX2-1.^{3,4} Although

intensified chemotherapy regimens have significantly improved survival rates, relapse remains a major challenge and is often associated with a poor prognosis. Furthermore, aggressive chemotherapy regimens are accompanied by severe short- and long-term side effects.^{5,6} Therefore, understanding the molecular mechanisms underlying T-ALL is crucial for developing more effective treatments and improving patient outcomes and quality of life.

While advances in molecular biology have provided valuable insights into the genetic basis of T-ALL, the intricate regulatory mechanisms governing its pathogenesis are still not completely understood. Unlike other leukemias, T-ALL

and B-cell lymphoblastic leukemia (B-ALL) exhibit few or no mutations affecting splicing factors (SF).^{3,7} However, previous studies have revealed widespread changes in their splicing landscapes, even in the absence of SF mutations. These changes are attributed to post-transcriptional or post-translational dysregulation of SF.⁸⁻¹⁰

Recently, attention has turned towards the role of RNA-binding proteins (RBP) in orchestrating post-transcriptional processes that drive oncogenic transformation. Among the diverse array of RBP, the Quaking protein (QKI), a member of the Signal Transduction and Activation of RNA (STAR) family of RBP, plays a pivotal role in various cellular processes through its regulation of RNA metabolism.¹¹ Previous studies have identified decreased *QKI* expression, along with increased expression of *HOXA* genes, as among the most significantly differentially expressed genes in T-ALL patients with MLL-rearrangements, and *SET-NUP214* and *CALM-AF10* translocations compared to other T-ALL subgroups.¹²⁻¹⁵ Additionally, we have linked reduced *QKI* expression to circular RNA dysregulation in T-ALL, underscoring its multifaceted role in leukemia biology.¹⁶

QKI is encoded by the *QKI* gene and is involved in the regulation of mRNA splicing, stability, translation, and localization.¹¹ The functional diversity of *QKI* is largely attributed to the presence of multiple isoforms, which arise from alternative splicing of its pre-mRNA.¹⁷ These isoforms include QKI-5, QKI-6, and QKI-7, each of which differs in its C-terminal region, exhibiting distinct subcellular localizations and functions.¹¹ QKI-5 is predominantly nuclear and is implicated in the regulation of alternative splicing,^{18,19} a process in which non-coding regions called introns are excised from pre-mRNA molecules, and the remaining coding regions, known as exons, are joined together. QKI-5 interacts with specific RNA sequences, known as Quaking response elements (QRE) to influence the splicing of pre-mRNA involved in various cellular pathways.²⁰ This isoform is particularly important during developmental processes, such as myelination in the central nervous system, where it regulates the splicing of mRNA essential for oligodendrocyte maturation and function.²¹ Additionally, QKI-5 has been shown to play a role in epithelial-mesenchymal transition (EMT), a process crucial for cancer metastasis, by modulating the splicing of mRNA that contribute to the mesenchymal phenotype.²²⁻²⁴ Dysregulation of *QKI* expression has been implicated in various pathological conditions, including neurodevelopmental disorders, cardiovascular diseases, and cancer.^{22,25-27}

Here, we investigated the expression of *QKI* in two large, independent pediatric T-ALL cohorts. Our analysis demonstrated that *QKI* expression was decreased in T-ALL patients compared to their healthy counterparts (thymocytes). Additionally, silencing *QKI* in T-ALL cell lines allowed us to identify the pool of *QKI*-regulated splicing events, which were subsequently confirmed to be dysregulated in T-ALL patients with lower *QKI* expression levels. Furthermore,

QKI expression in primary samples was highly correlated with the degree of missplicing. Through *in vivo* studies, we demonstrated that *QKI* overexpression prolongs survival and significantly reduces leukemic infiltration in multiple organs, highlighting its tumor-suppressive potential in the T-ALL models tested. In conclusion, we characterized *QKI* as an RNA-binding protein with tumor suppressive properties in T-ALL and defined the dysregulated splicing landscape associated with its loss, laying the groundwork for the discovery of new therapeutic targets and prognostic markers.

Methods

Cell lines

T-cell acute lymphoblastic leukemia cell lines were cultured in RPMI 1640 medium supplemented with 20% (HPB-ALL and KARPAS-45) or 10% (Jurkat, DND-41, TALL-1, LOUCY, ALL-SIL, KOPT-K1, PF-382) fetal calf serum (FCS), 100 U/mL penicillin, 100 mg/mL streptomycin, and 2 mM L-glutamine at 37°C with 5% CO₂. HEK293 cells were cultured in DMEM supplemented with 10% fetal calf serum, 100 U/mL penicillin, 100 mg/mL streptomycin, and 2 mM L-glutamine at 37°C with 5% CO₂.

Primary samples

De-identified primary patient samples were obtained from the Children's Oncology Group ALL0434 study and the University of New Mexico (Institutional Review Board numbers 16-246 and 03-183). All patients or their parents or guardians provided written, informed consent in accordance with the Declaration of Helsinki and local institutional guidelines.

In vivo mouse experiments

NOD.Cg-Prkdcscid Il2rgtm1Wjl/SzJ (NSG) 6-8-week old mice were purchased from the Jackson Laboratory and maintained in a pathogen-free, AAALAC-accredited facility. The animal experiments were approved by the Ethical Committees on animal welfare at the University of Alabama at Birmingham (IACUC-22544, IACUC-22519). The T-ALL cell lines, PF-382 and KARPAS-45, were transduced with either a control construct or a *QKI* expression construct. A total of 10⁶ transduced T-ALL cells were injected into the tail vein of each mouse. For survival analyses, mice (N=10 per group) were euthanized upon showing signs of moribund disease and/or a weight loss of 15%. For leukemia burden analyses, animals (N=5 per group) received 10⁶ transduced PF-382 or KARPAS-45 cells via tail vein injection. All mice were sacrificed at the same time point: 23 days for PF-382 and 32 days for KARPAS-45 post engraftment. Leukemic cells were isolated from the bone marrow of femurs, blood, meninges, spleen, liver, and lungs. Cells were stained using anti-human APC-CD45 and anti-mouse BV-421-CD45 antibodies (BD Biosciences) and analyzed by flow cytometry. Data were processed using FlowJo software.

RNA sequencing

RNA integrity was assessed and sequenced using Illumina Truseq stranded total RNA library prep (150 bp paired-end). Sequenced reads were trimmed for adapter sequences and low-quality bases using TRIMMOMATIC v0.39. Trimmed sequence reads were aligned to the human genome using STAR v2.7.11b and quantified at the transcriptome level using Salmon v1.10.3 using GRCh38 Gencode release 44 reference. Differential gene expression analysis was performed using DESeq2. GSEA was performed using Hallmark²⁸ gene set collections. Splicing analysis was carried out using MAJIQ v2.5.7.²⁹ The heterogen module was applied to primary samples, while splicing changes in cell lines were analyzed using MAJIQ DeltaPsi. For each local splicing variant (LSV), MAJIQ calculates the mean percent spliced in (PSI, ψ) to determine the delta PSI ($\Delta\psi$) between two groups. LSV with a $\Delta\psi > 0.15$ (15%) and a probability of change > 0.95 were considered changing and subjected to further analysis. Changing LSV were then aggregated into modules using VOILA modularize to facilitate biological interpretation of alternative splicing events. Further information on the methods used is available in the *Online Supplementary Methods*.

Results

QKI is down-regulated in T-cell acute lymphoblastic leukemia

Given that dysregulated splicing is common in T-ALL^{9,30} and that *QKI* has a critical role in splicing,^{18,19} we explored *QKI* gene expression in primary T-ALL samples. We analyzed publicly available RNA-Seq data from two independent pediatric patient cohorts, TARGET (N=265)³ and Verboom et al. (N=60),³¹ alongside healthy thymocytes from different developmental stages.³² These cohorts provide comprehensive transcriptional profiles of primary T-ALL samples, enabling robust comparisons with healthy thymocytes at various developmental stages. Overall, T-ALL blasts exhibited lower *QKI* mRNA expression compared to healthy thymocytes (Figure 1A). We next investigated whether low *QKI* expression is associated with any of the T-ALL molecular subgroups. Interestingly, T-ALL patient samples within the HOXA subgroup showed significantly lower *QKI* mRNA expression than the other subgroups (Figure 1B). In addition, analysis of a recently published T-ALL dataset with a more refined molecular subtype classification³³ revealed that *QKI* expression is significantly reduced in the NUP98, LMO2 $\delta\gamma$ -like, MLLT10, KMT2A, and NUP214 subtypes (*Online Supplementary Figure S1A*). T-ALL can arise from the blockade of normal T-cell development, which prompted us to investigate *QKI* expression during this process. We observed that *QKI* expression remains relatively stable across all stages of normal T-cell development (*Online Supplementary Figure S1B*). In contrast, the significantly reduced

QKI expression observed in T-ALL deviates from this steady expression pattern, suggesting that low *QKI* levels are an abnormal feature of T-ALL rather than a reflection of normal developmental variation. Using a Cox proportional-hazards model, we assessed the relationship between *QKI* expression and overall survival of T-ALL patients in the TARGET cohort. Patients with lower *QKI* mRNA expression had worse overall survival ($P=0.018$) and event-free survival ($P=0.053$) compared to those with high *QKI* expression (Figure 1C, *Online Supplementary Figure S1C*). To assess which *QKI* isoforms are expressed in normal T cells, we inspected the 3' end of *QKI* transcripts using both long-read sequencing (ONT) and short-read sequencing (Illumina) RNA-Seq data. We predominantly identified reads that were consistent with the *QKI*-5 transcript (*Online Supplementary Figure S1D*). To further identify the presence of *QKI* protein isoforms, we performed western blotting with *QKI*-specific antibodies (anti-*QKI*-5, anti-*QKI*-6, anti-*QKI*-7, and anti-*QKI*-7B) as well as an antibody that targets all *QKI* isoforms (anti-Pan-*QKI*). Our results showed that only the *QKI*-5 protein was detected (*Online Supplementary Figure S1E*). To establish whether T-ALL patients exhibit decreased *QKI* protein levels, we tested a set of primary patient samples. Our findings revealed that, among the 9 patient samples examined, 5 had low *QKI* protein levels, all of which belonged to the HOXA subtype (Figure 1D). Two additional HOXA cases exhibited higher *QKI* expression. Decreased *QKI* expression in T-ALL samples prompted us to examine *QKI* mutations and copy number variations (CNV) in the TARGET cohort. We identified 8 patients with *QKI* CNV, of which 5 were copy number losses and 3 were copy number gains (*Online Supplementary Figure S1F*). Moreover, there were no *QKI* mutations reported in this dataset. Thus, *QKI* dysregulation cannot be attributed solely to genetic mutations, suggesting that other factors are involved.

Next, we explored *QKI* expression in T-ALL cell lines by analyzing RNA-Seq data from a panel of 13 T-ALL cell lines, which included both publicly available datasets^{34,35} and in-house sequenced cell lines. Upon examining *QKI* mRNA levels, we found that LOUCY and KARPAS-45 expressed the lowest levels of *QKI*, while HPB-ALL and TALL-1 exhibited high *QKI* expression (Figure 1E). Our results are consistent with a previous study in which reduced *QKI* expression in the LOUCY cell line was associated with the *SET-NUP214* fusion and elevated *HOXA* gene expression.¹² KARPAS-45 is an MLL-rearranged cell line and is also associated with high *HOXA* expression.

Transcript expression does not always result in equivalent protein abundance. Therefore, we assessed *QKI* protein levels using western blotting and mass spectrometry, generating matched RNA-Seq and proteomics data for 6 T-ALL cell lines (LOUCY, KARPAS-45, DND-45, HPB-ALL, ALL-SIL, TALL-1). Linear regression analysis revealed a strong correlation between *QKI* mRNA and protein abundance ($R^2=0.8552$, $P < 0.001$) (Figure 1F). Immunoblotting using

a QKI-5 specific antibody confirmed that QKI-5 is almost absent in the T-ALL cell lines LOUCY and KARPAS-45 (Figure 1G). The high correlation observed between mRNA and

protein suggests that *QKI* expression is mainly regulated at the transcriptional level. Given that T-ALL cases exhibit reduced *QKI* expression compared to their natural counter-

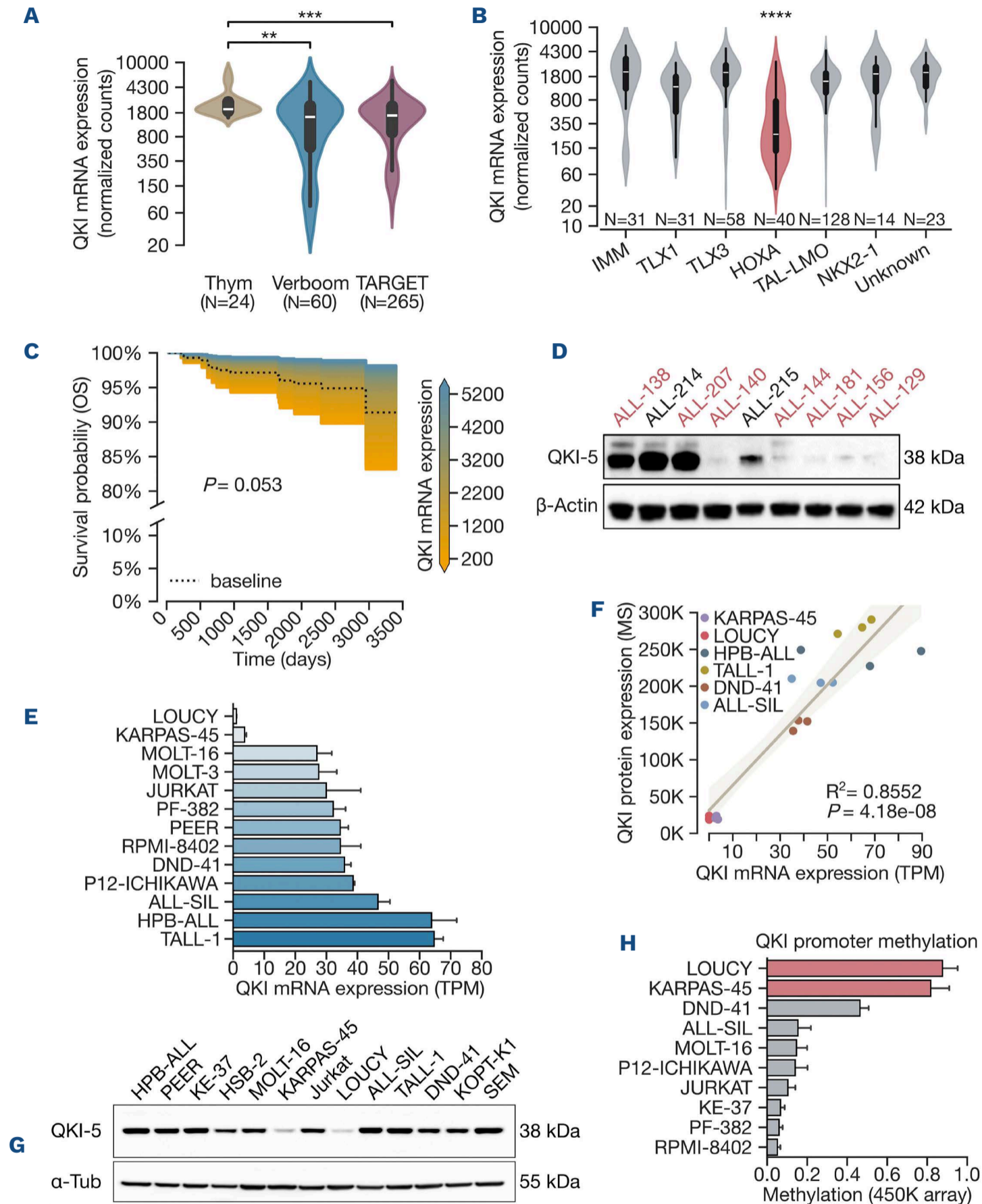


Figure 1. T-cell acute lymphoblastic leukemia patients exhibit low Quaking protein expression. (A) Box plots of Quaking (*QKI*) protein mRNA expression showing that T-cell acute lymphoblastic leukemia (T-ALL) patients from two independent cohorts (Verboom and TARGET) exhibit low *QKI* expression when compared to healthy thymocytes. $**P < 0.01$; $***P < 0.001$; unpaired Mann-Whitney U test. (B) Box plots of *QKI* expression grouped by T-ALL molecular subtypes. $****P < 0.0001$; Kruskal-Wallis with Dunn's post-hoc test. (C) Survival plot of patients from the TARGET cohort representing overall survival probabilities according to *QKI* expression using a Cox proportional-hazards model. The dashed line represents the baseline (average *QKI* expression). Patients with low *QKI* expression present a worse prognosis when compared to patients with high *QKI* high levels. (D) *QKI* protein levels in primary T-ALL patients determined by western blotting. HOXA group samples are shown in red. (E) mRNA expression of *QKI* in a panel of T-ALL cell lines. (F) Linear regression plot showing the correlation between *QKI* mRNA and protein levels in 6 T-ALL cell lines. (G) Western blot showing *QKI*-5 protein expression in a panel of 13 T-ALL cell lines. (H) *QKI* promoter methylation status determined by Illumina 450K BeadChip array.⁴⁰

part and that *QKI* genetic abnormalities are mostly absent in primary T-ALL samples, we hypothesized that epigenetic mechanisms might be responsible for the low *QKI* levels observed in T-ALL patients. It was shown that epigenetic alterations in T-ALL play a crucial role in regulating gene expression and cellular processes, leading to the silencing of tumor suppressor genes or the activation of oncogenes,

which promote cell proliferation and survival.³⁶ Interestingly, hierarchical clustering of gene expression data from the TARGET cohort revealed that *QKI* and *TET2* display similar expression patterns (*Online Supplementary Figure S1F*). Given that *TET2* expression is silenced in T-ALL through promoter hypermethylation,^{37,38} we investigated whether a similar mechanism underlies the regulation of *QKI* by exam-

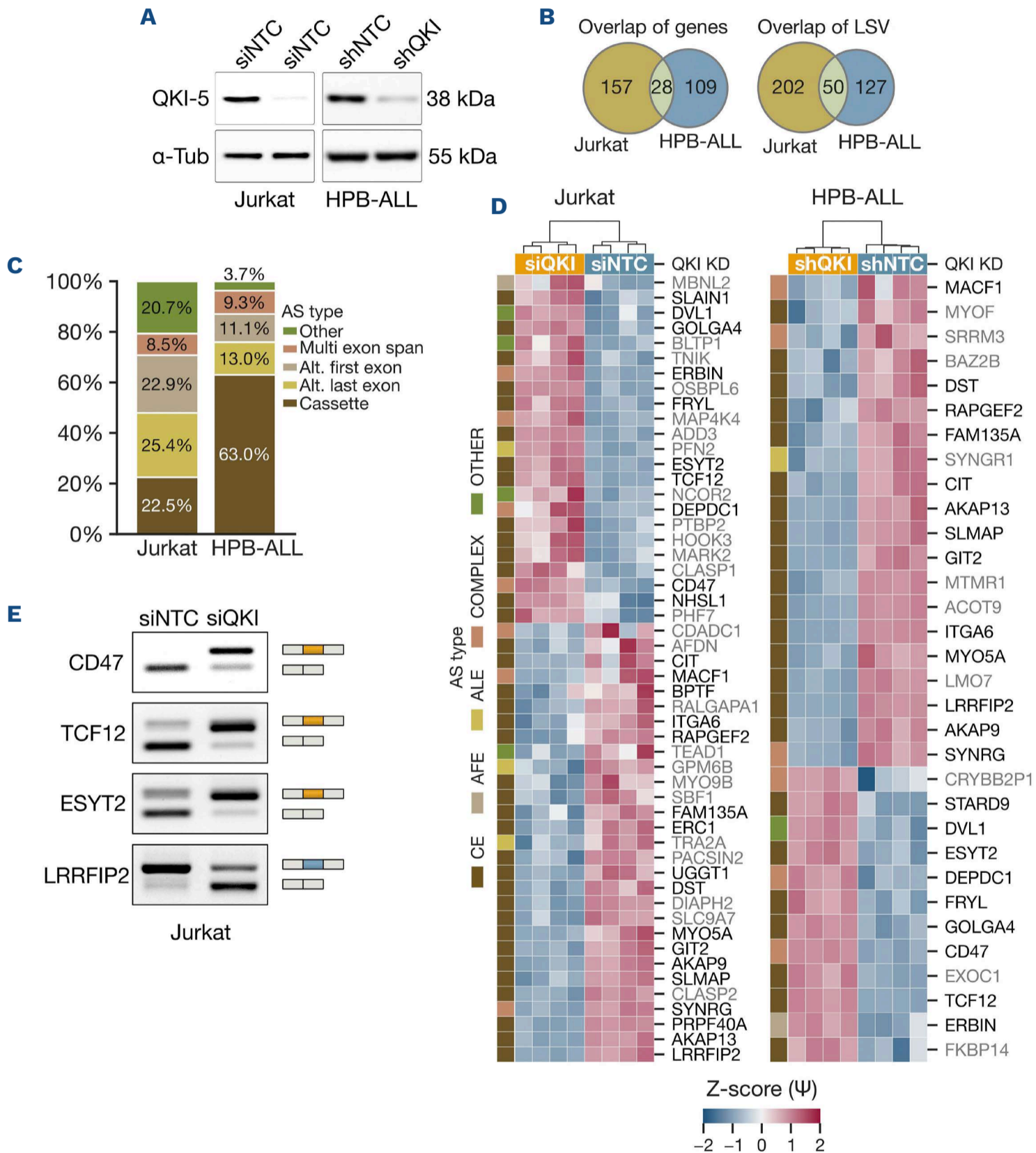


Figure 2. Quaking protein depletion leads to altered mRNA splicing in T-cell acute lymphoblastic leukemia cell lines. (A) Western blot analysis confirming Quaking (QKI) protein knockdown in Jurkat and HPB-ALL cells using siRNA (siQKI) and shRNA (shQKI), respectively. α -Tubulin was used as a loading control. (B) Venn diagrams showing the overlap of local splicing variants (LSV) and genes affected by QKI knockdown in Jurkat and HPB-ALL cells. (C) Distribution of splicing event types upon QKI knockdown in Jurkat and HPB-ALL cells. (D) Heatmap of splicing changes (Z-score of ψ) in select genes across Jurkat and HPB-ALL cells upon QKI depletion, demonstrating both inclusion and skipping of exons in various transcripts. Genes in darker shade represent splicing changes detected in both Jurkat and HPB-ALL. (E) Real-time polymerase chain reaction validation of QKI-dependent splicing events in Jurkat cells for CD47, ESYT2, and TCF12 transcripts, showing exon inclusion/skipping upon QKI knockdown. The higher band represents the inclusion of the cassette exon whereas the smaller band represents the exclusion.

ining the methylation status of the *QKI* promoter in T-ALL cell lines. Genome-wide DNA methylation data from T-ALL cell lines³⁹ revealed that the *QKI* promoter is hypermethylated in both KARPAS-45 and LOUCY cell lines compared to other T-ALL cell lines (Figure 1H, *Online Supplementary Figure S1G*), suggesting a potential epigenetic mechanism for *QKI* dysregulation.

Taken together, our results demonstrate a significant reduction in *QKI* expression in T-ALL blasts compared to healthy thymocytes, particularly in the HOXA subgroup. This reduction in *QKI* expression is associated with a worse outcome in T-ALL patients. Data from T-ALL cell lines further support a strong correlation between *QKI* mRNA and protein levels.

***QKI* depletion leads to altered mRNA splicing in T-cell acute lymphoblastic leukemia cell lines**

To characterize the impact of low *QKI* expression levels in the T-ALL splicing landscape, we silenced the main T-ALL-expressed *QKI* isoform, *QKI*-5, in JURKAT and HPB-ALL cells, which exhibit medium to high *QKI* expression. We established two models for transient and stable depletion of *QKI* expression by siRNA-mediated knockdown in Jurkat cells and shRNA-mediated knockdown in HPB-ALL cells. Assessment of the knockdown efficiency by western blotting showed a robust decrease in *QKI* protein abundance in both tested cell lines (Figure 2A). Subsequently, total RNA was extracted and processed for RNA-sequencing to identify changes in mRNA splicing upon *QKI* depletion.

We then used MAJIQ v2²⁹ to perform differential splicing analysis on the RNA-Seq data obtained from each cell line. For each local splicing variant (LSV) a mean percent spliced in (PSI, ψ) value was calculated and groups were compared using the delta PSI ($\Delta\psi$) metric. LSV with a $\Delta\psi > 0.15$ (15%; 5% FDR) were considered differentially spliced and further analyzed. A total of 252 differentially spliced LSV were identified in Jurkat cells when comparing si*QKI* with siNTC, while 177 were altered when comparing sh*QKI* with shNTC in HPB-ALL cells. These LSV involved 185 and 137 genes in Jurkat and HPB-ALL, respectively. The analysis of the splicing changes in Jurkat and HPB-ALL cells revealed that although some events were unique to each cell line, 50 LSV (28 genes) were common to both cell lines (Figure 2B).

To help interpret the biological implications of the splicing changes, LSV were aggregated into alternative splicing modules (the combination of possible splicing events), and the most relevant differentially spliced event was extracted. Among all the event types detected, alternative last exon events were the most commonly impacted by *QKI* depletion in Jurkat cells (22.5%), followed by alternative first exon (22.9%) and cassette exon (22.5%) events, whereas in HPB-ALL cells, cassette exon events were the most impacted (63.0%), followed by alternative last exon events (13.0%) (Figure 2C).

Splicing factors, such as *QKI*, have been shown to either promote or inhibit splice site recognition, depending on their binding sequence context.²⁹ Therefore, to understand

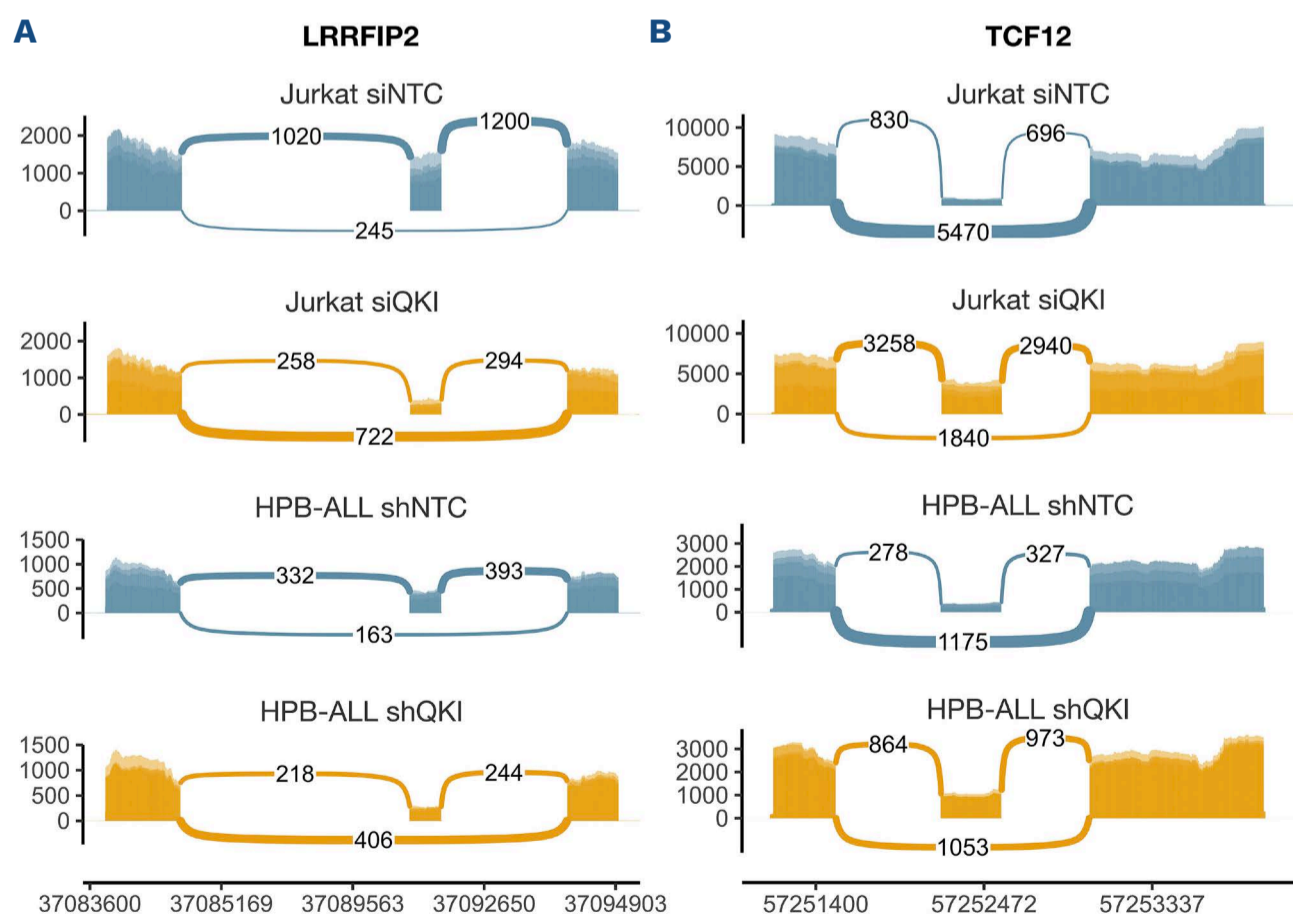


Figure 3. Quaking protein-dependent exon usage in *LRRFIP2* and *TCF12*. Sashimi plots depicting Quaking (*QKI*) protein-dependent splicing changes in *LRRFIP2* (A) and *TCF12* (B). The plots illustrate exon skipping/inclusion events in both Jurkat and HPB-ALL cells, as visualized through RNA-seq data.

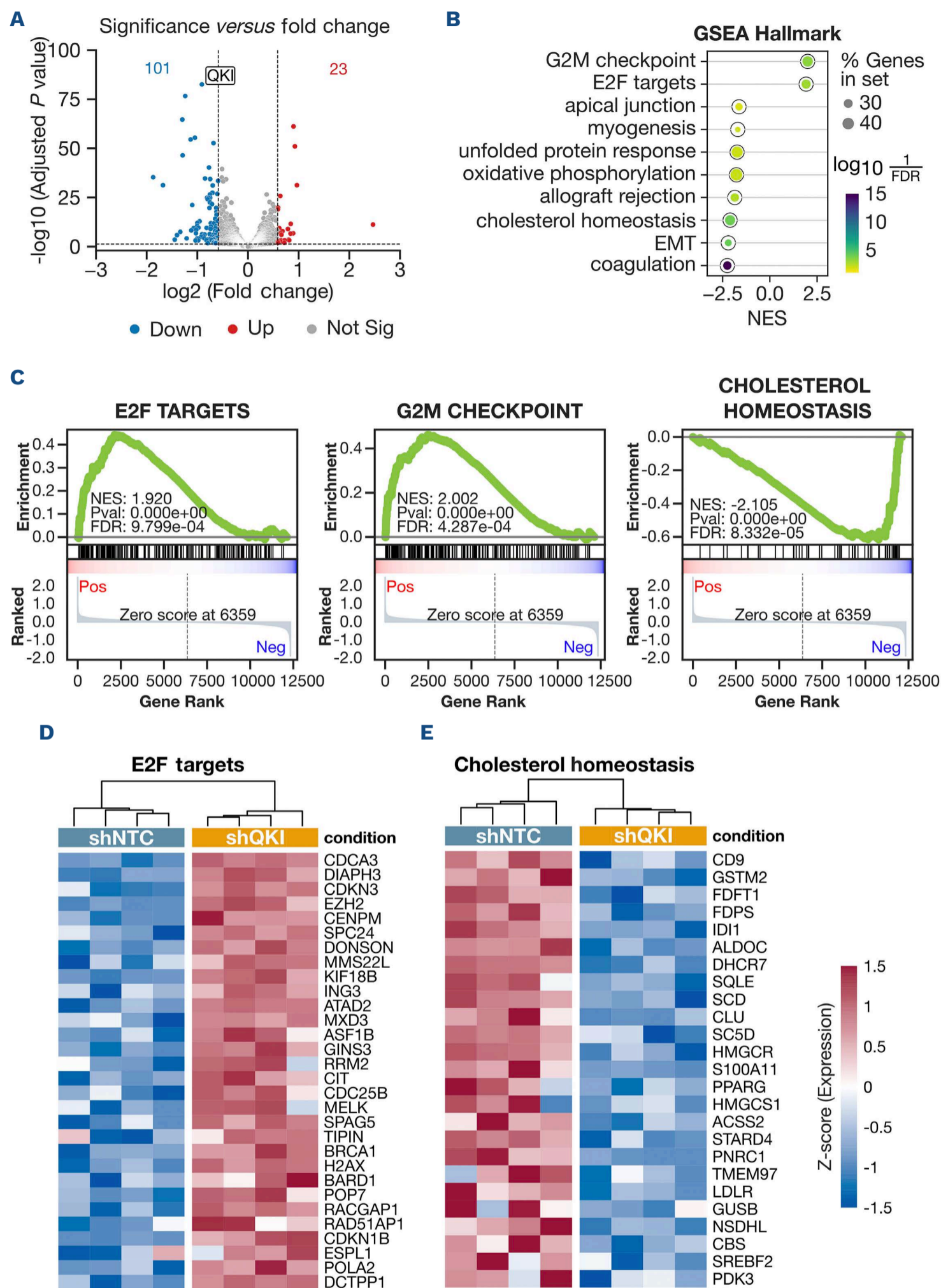


Figure 4. Quaking protein silencing induces widespread transcriptional changes in T-cell acute lymphoblastic leukemia cells.

(A) Volcano plot illustrating differentially expressed genes in HPB-ALL cells transduced with shQKI compared to shNTC. A total of 23 genes were significantly up-regulated, while 101 were down-regulated (absolute fold change >1.5, $P < 0.05$). (B) Gene Set Enrichment Analysis (GSEA) showing positive enrichment for the gene sets of E2F targets, G2M checkpoint, and negative enrichment for cholesterol homeostasis, epithelial-to-mesenchymal transition (EMT) and coagulation. (C) GSEA plots depicting the enrichment scores for E2F targets, G2M checkpoint, and cholesterol homeostasis. (D and E) Heatmaps displaying the top differentially expressed genes contributing to the GSEA signature for the E2F targets (top 30; D) and cholesterol homeostasis (top 25; E) gene sets, showing significant upregulation and downregulation, respectively, upon Quaking (QKI) protein silencing.

the directional changes in splicing events affected by *QKI* depletion, we extracted and analyzed the ψ values (inclusion level) for each sample across alternatively spliced events. As expected, Jurkat and HPB-ALL samples clustered according to the presence or absence of *QKI*. More importantly, two distinct splicing patterns were observed within each cell line upon *QKI* depletion: one cluster of splicing events with increased inclusion, and another with increased skipping

(Figure 2D). Among the 52 differentially spliced modules, 23 (44%) showed increased inclusion following *QKI* depletion in Jurkat cells, whereas 29 (56%) showed increased skipping. Similarly, 12 out of 32 (37%) differentially spliced modules were included upon *QKI* knockdown, whereas 20 (63%) were skipped in HPB-ALL. To validate the detected splicing events, we performed independent RT-PCR on a subset of representative events using primers flanking the

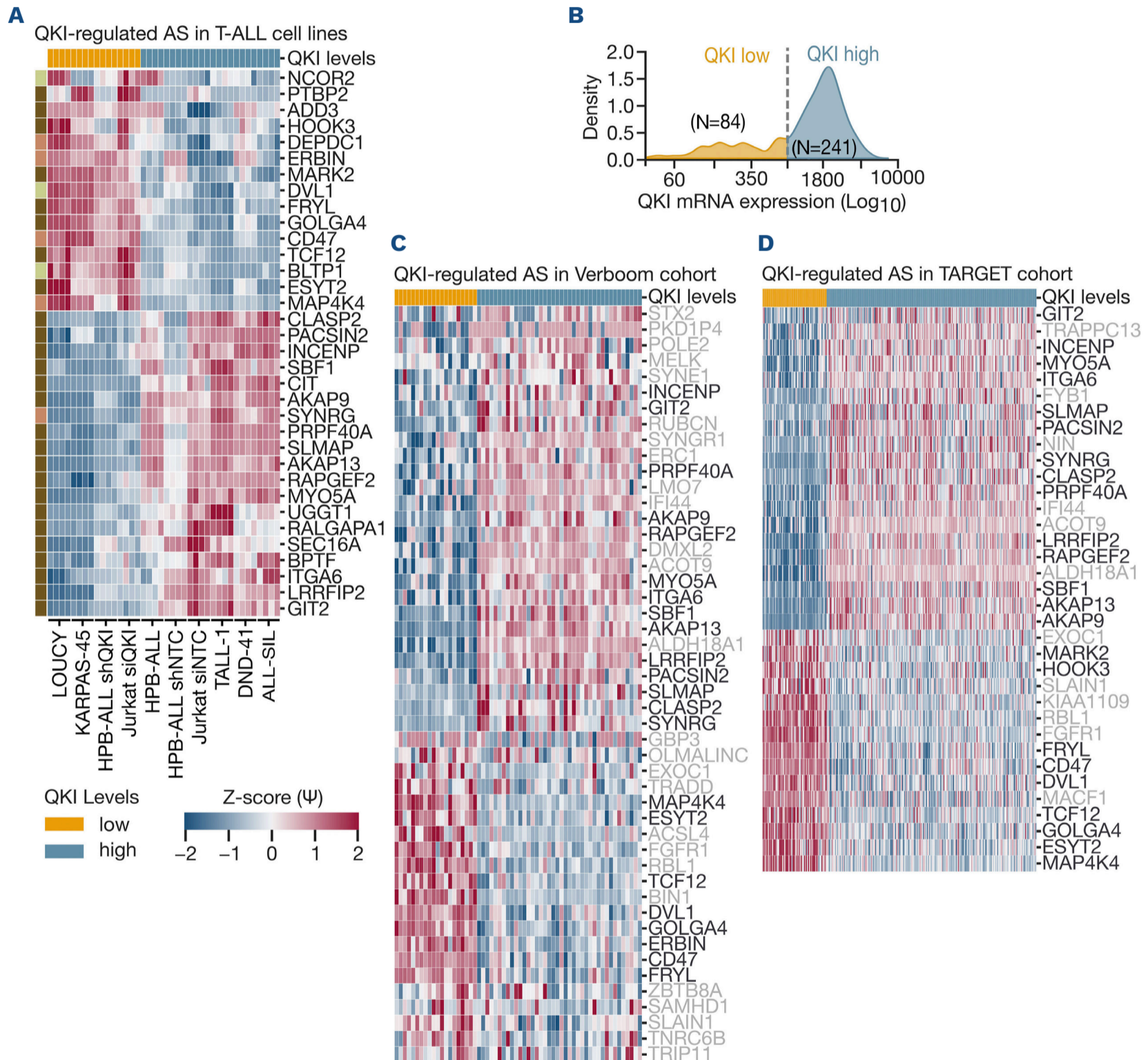


Figure 5. Splicing changes detected in T-cell acute lymphoblastic leukemia cell lines are corroborated in primary T-cell acute lymphoblastic leukemia samples. (A) Heatmap of splicing patterns in T-cell acute lymphoblastic leukemia (T-ALL) cell lines with low Quaking (*QKI*) protein expression, *KARPAS-45* and *LOUCY* alongside *Jurkat* and *HPB-ALL* cells where *QKI* was experimentally silenced and cells lines with high *QKI* expression. Cell lines with higher *QKI* expression formed a separate cluster, highlighting a common splicing signature driven by *QKI* levels. (B) Kernel density estimation (KDE) plot showing the distribution of *QKI* mRNA expression in T-ALL patient samples (both cohorts). The horizontal dashed line represents the cutoff (800) for the stratification of *QKI*-high and *QKI*-low, depending on whether patients have *QKI* expression above or under the cutoff, respectively. (C and D) Heatmaps representing the PSI (Ψ) values of *QKI*-regulated splicing events for each patient in the Verboom (C) and TARGET (D) cohorts, confirming that many splicing changes observed in cell lines are also consistently altered in both patient cohorts, according to *QKI* expression levels. Genes in darker shade represent concordant splicing changes detected in both primary cohorts and in T-ALL cell lines.

alternatively spliced cassette exons, confirming the splicing patterns identified in the computational analysis (Figure 2E). To further corroborate these findings, we performed siRNA-mediated depletion of *QKI* in an additional T-ALL cell line with high *QKI* levels, ALL-SIL, and validated the changes observed upon *QKI* loss in Jurkat and HPB-ALL cells (Online Supplementary Figure S2).

We identified previously known *QKI* targets in solid tumors, including *ADD3*,²⁶ *CD47*, *DEPDC1*²³ and *ESYT2*,^{22,24} *AKAP9*²⁷ as well as novel *QKI*-regulated splicing events specific to T-ALL, such as *ERBIN*, *DVL1* and *TCF12*. For example, *QKI* knockdown led to exon inclusion in transcripts of the cell surface “don’t eat me” signal *CD47*, extended synaptotagmin 2 (*ESYT2*), the Wnt/ β -catenin signaling pathway component *DVL1* and the T-cell transcription factor *TCF12* (also known as *HEB*) (Figure 3A), suggesting that *QKI* represses the inclusion of these exons. Conversely, *QKI*-depleted cells exhibited exon skipping in the Wnt/ β -catenin signaling pathway component *LRRFIP2*, indicating that *QKI* positively regulates the inclusion of this exon in the mature transcript (Figure 3B). Taken together, the data presented here show that *QKI* modulates specific splicing events in T-ALL, which may contribute to its biological functions.

Downregulation of *QKI* induces global transcriptional alterations in T-cell acute lymphoblastic leukemia

Next, we sought to characterize the transcriptional land-

scape on *QKI* silencing in T-ALL cells. We performed differential gene expression (DGE) analysis between sh*QKI* and shNTC transduced HPB-ALL cells. A total of 23 genes were found to be significantly up-regulated, while 101 genes were down-regulated (absolute fold change >1.5, $P < 0.05$) (Figure 4A).

To unravel the biological implications of the differentially expressed genes, we ranked them by log₂ fold change and performed Gene Set Enrichment Analysis (GSEA) using the hallmark gene sets from MSigDB.^{28,40} The results showed a strong positive enrichment for the gene sets of E2F targets and G2M checkpoint. Conversely, there was a negative enrichment for the cholesterol homeostasis, the epithelial to mesenchymal transition and coagulation gene sets (Figure 4B). The visualization of the GSEA plots revealed a clear profile with the up-regulated genes driving the positive enrichment score associated with the E2F targets and G2M checkpoints gene sets. Conversely, down-regulated genes contributed to the negative enrichment score of the cholesterol homeostasis (Figure 4C) and coagulation gene sets (Online Supplementary Figure S3A). Moreover, we investigated the GSEA enrichment of the EMT gene set, a process that has been shown to be influenced by *QKI* expression.^{23,24} As expected, we observed an association between down-regulated genes and the EMT signature (Online Supplementary Figure S3A).

To gain further insights into the genes contributing to the

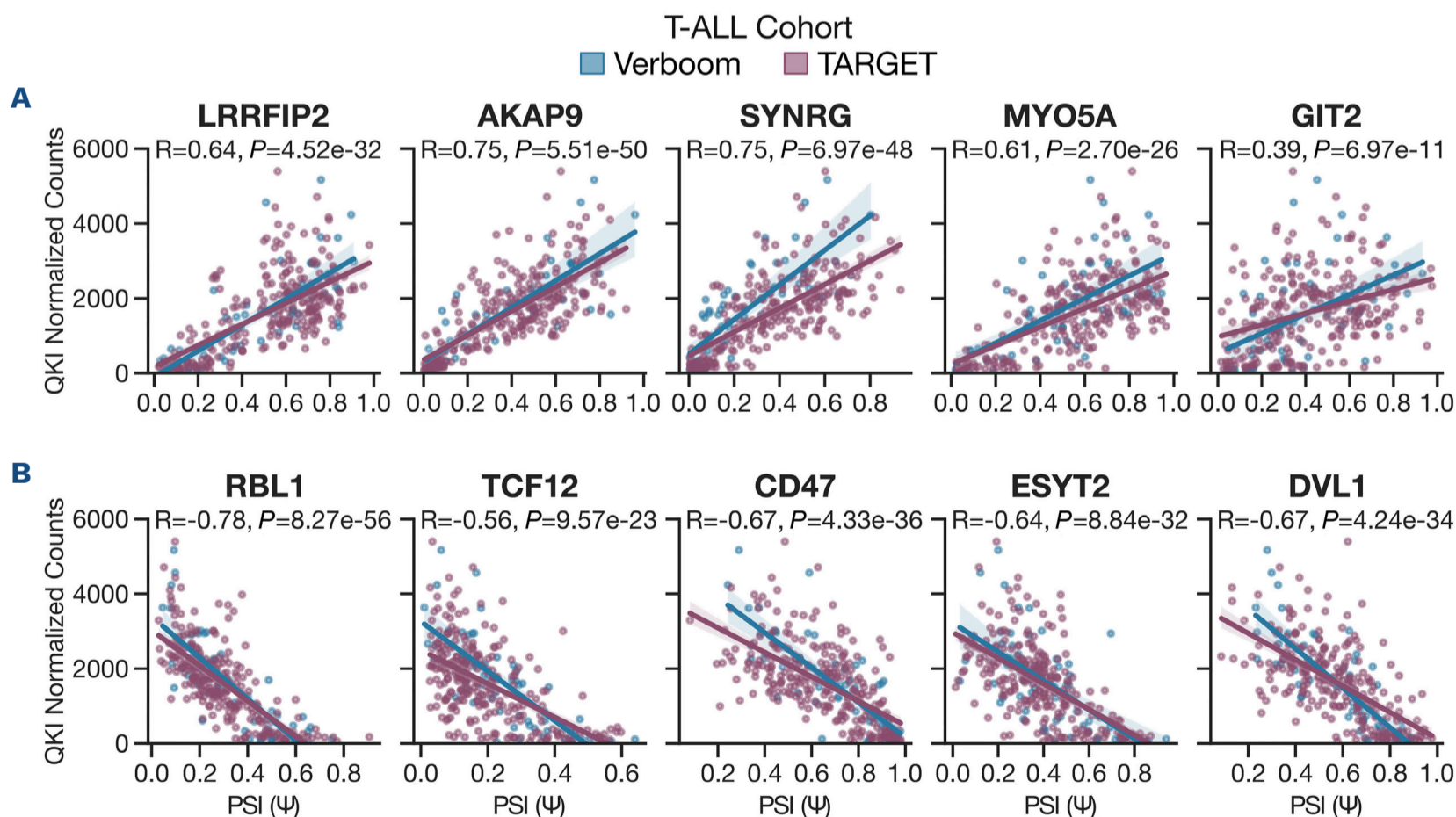


Figure 6. Correlation between Quaking protein expression and alternative splicing across T-cell acute lymphoblastic leukemia patient cohorts. Linear regression plots depicting the correlation between Quaking (*QKI*) protein expression and the PSI (ψ) values for selected splicing events across patients from each T-cell acute lymphoblastic leukemia (T-ALL) cohort. (A) Positive correlations events. (B) Negative correlations are events. The Spearman correlation coefficient and corresponding P value between PSI (ψ) and *QKI* counts from the TARGET cohort are provided for each gene.

positive enrichment of E2F targets, we explored the gene expression of the leading genes identified through GSEA analysis. A hierarchical clustering heatmap revealed a clear

difference in gene expression between shNTC and shQKI HPB-ALL cells. Among the top up-regulated genes were *SPC24*, *RRM2*, *CIT*, and *EZH2*, which all contribute to this

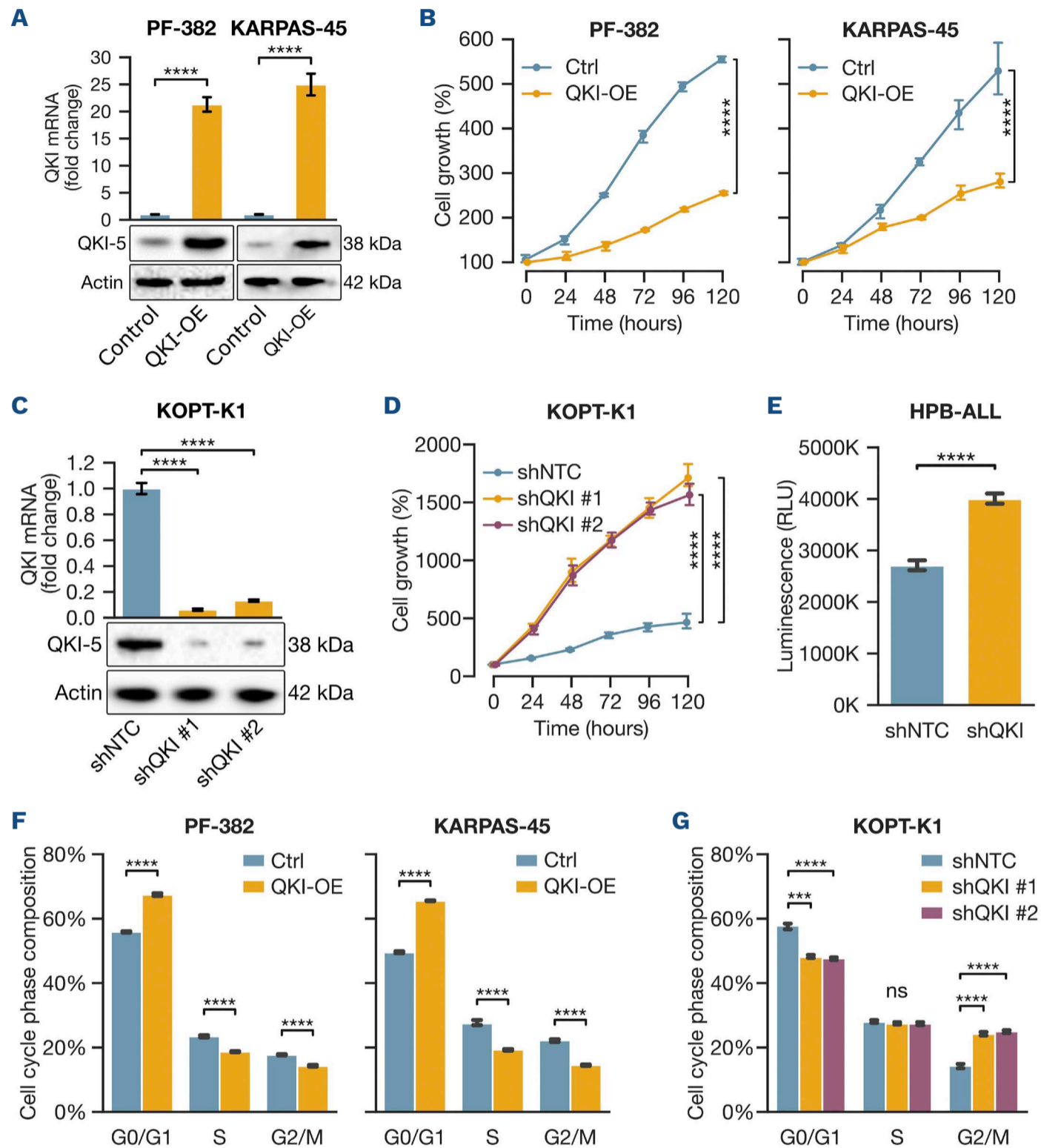


Figure 7. Quaking protein regulates proliferation and cell-cycle progression in T-cell acute lymphoblastic leukemia cells. (A) Quantitative polymerase chain reaction (PCR) (top) showing a significant increase in Quaking (QKI) protein mRNA levels in PF-382 and KARPAS-45 cells transduced with a QKI expression construct (QKI-OE) compared to the control construct, and western blot (bottom) confirming elevated QKI-5 protein levels. β -actin served as the loading control. (B) Cell proliferation curves showing reduced growth of PF-382 and KARPAS-45 cells over-expressing QKI compared to controls over a time course of 120 hours. Data are presented as the percentage of cell growth relative to the control. **** $P < 0.0001$; repeated measure ANOVA with Tukey's multiple comparisons test. (C) Quantitative PCR (top) showing efficient depletion of QKI mRNA in KOPT-K1 cells transduced with two independent shRNA targeting QKI (shQKI #1 and shQKI #2) compared to a non-targeting shRNA (shNTC), and corresponding western blot (bottom) confirming the reduced QKI-5 protein levels. β -actin served as the loading control. (D) Cell proliferation curves showing increased growth of QKI-depleted KOPT-K1 cells compared with controls over 120 hours. Data are presented as the percentage of cell growth relative to the control. **** $P < 0.0001$; repeated measure ANOVA with Tukey's multiple comparisons test. (E) Luminescence-based proliferation assay showing significant increased cell growth in QKI-depleted HPB-ALL cells compared to shNTC after 96 hours. **** $P < 0.0001$; unpaired Student *t* test. (F) Cell cycle analysis by flow cytometry showing a significant increase in the percentage of cells arrested in the G0/G1 phase in QKI-over-expressing PF-382 and KARPAS-45 cells, compared to control cells. **** $P < 0.0001$; unpaired Student *t* test. (G) Cell cycle analysis by flow cytometry showing a significant reduction of QKI-depleted KOPT-K1 cells in the G0/G1 phase compared with control cells. *** $P < 0.001$; **** $P < 0.0001$; repeated measure one-way ANOVA with Tukey's multiple comparisons test.

transcriptional signature (Figure 4D). Consistent with the cholesterol homeostasis signature, core pathway genes were among the most down-regulated in sh*QKI* HPB-ALL cells, including *HMGCR*, *SQLE*, *SREBF2*, *LDLR* and *FDFT1*, indicating suppression of cholesterol biosynthesis and uptake (Figure 4E).

To decouple the effects of differential alternative splicing from differential gene expression, we examined the expression levels of genes that were alternatively spliced upon *QKI* depletion in HPB-ALL cells. Notably, most alternatively spliced genes showed no significant changes in overall expression (Online Supplementary Figure S3B). Therefore, the observed differential expression of transcripts following *QKI* depletion is likely to be an indirect effect, potentially mediated by some of the alternatively spliced genes rather

than through direct transcriptional regulation by *QKI*. Collectively, our findings showed that *QKI* silencing in T-ALL cells induce substantial changes in gene expression. These changes highlight the role of *QKI* in regulating key pathways related to cell proliferation and differentiation. Notably, alternative splicing and gene expression changes appear largely independent, suggesting that the influence of *QKI* on transcription may be indirect, potentially mediated through its regulation of splicing events.

***QKI* dysregulation induces ubiquitous aberrant splicing in T-cell acute lymphoblastic leukemia**

To confirm the splicing changes driven by *QKI* in a broader range of T-ALL cell lines we compared the splicing patterns associated with endogenous *QKI* levels in a panel of T-ALL

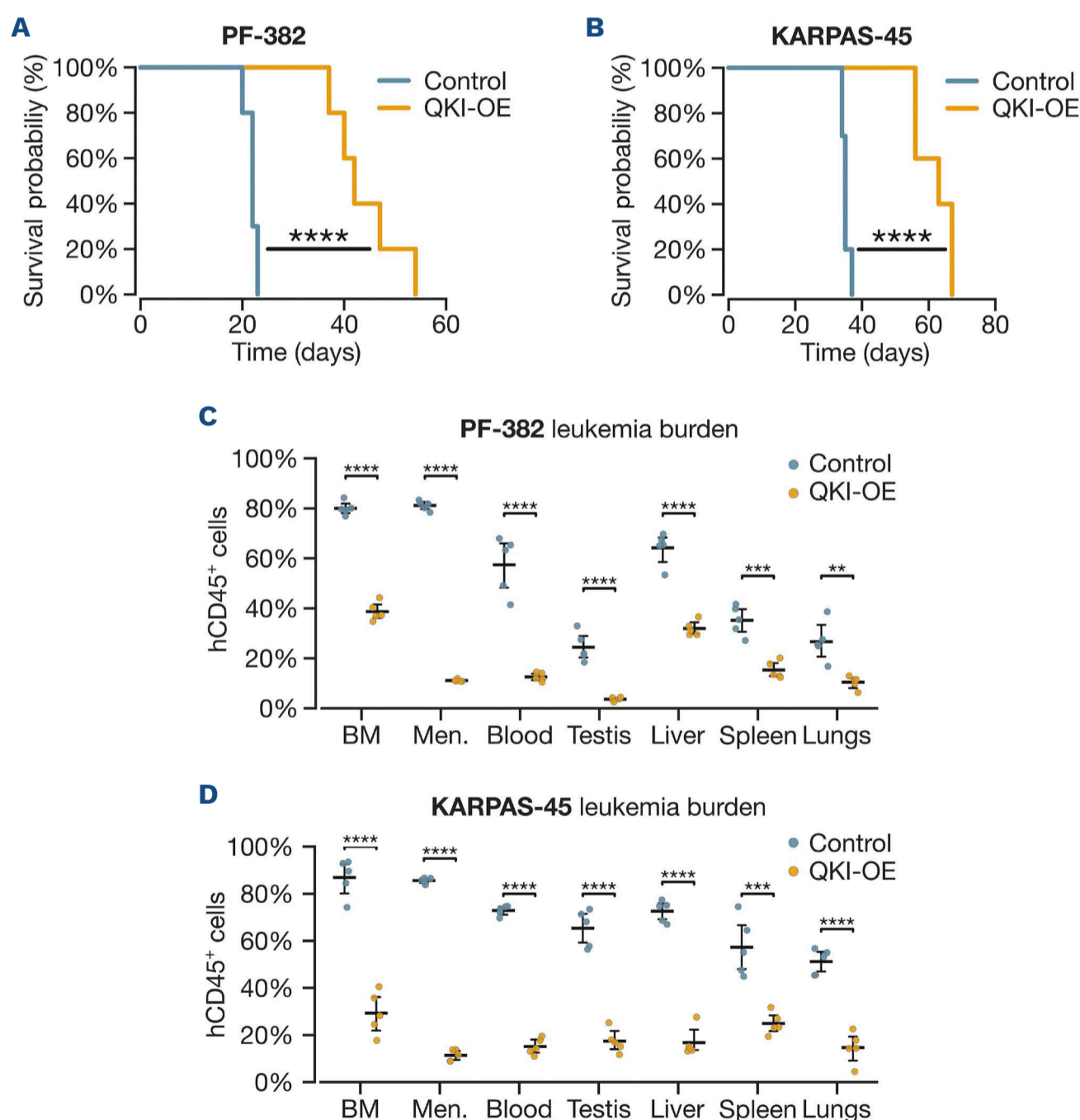


Figure 8. Quaking protein overexpression prolongs survival in T-cell acute lymphoblastic leukemia xenografts. Kaplan-Meier survival curve of NSG mice transplanted via tail vein with (A) PF-382 and (B) KARPAS-45 cells transduced to overexpress *QKI* (yellow) or control vector (blue) (10^6 cell/mouse), demonstrating that Quaking (*QKI*) protein overexpression prolongs animal survival. **** $P < 0.0001$; log-rank Mantel-Cox test. Leukemia burden was assessed at Day 23 for PF-382 and Day 32 for KARPAS-45 post engraftment, determined by the infiltration of human CD45⁺ cells in bone marrow (BM), meninges (Men.), blood, testis, liver, spleen, and lungs on NSG mice inoculated with (C) PF-382 and (D) KARPAS-45 transduced T-cell acute lymphoblastic leukemia (T-ALL) cells (10^6 cell/mouse via tail vein). ** $P < 0.01$; *** $P < 0.001$; **** $P < 0.0001$; unpaired Student *t* test with Holm-Sidak multiple comparison correction.

cell lines with those detected by experimental *QKI* silencing in HPB-ALL and Jurkat cells. The heatmap revealed that the splicing profiles of KARPAS-45 and LOUCY cells, which express low levels of *QKI*, displayed splicing patterns similar to those of Jurkat and HPB-ALL cells in which *QKI* was silenced, whereas cell lines with higher *QKI* expression exhibited distinct profiles. This further suggests that the splicing events detected by *QKI* silencing are a common feature related to endogenous *QKI* expression, since they were also detected in other T-ALL cell lines under normal conditions (Figure 5A).

Although cell lines are useful to study and model the molecular mechanisms of diseases, they may not always accurately reflect the characteristics of T-ALL patients. To overcome this, we performed differential splicing analysis using primary samples from two independent T-ALL cohort datasets: TARGET and Verboom. First, we stratified the patients according to their *QKI* expression level. Specifically, using the kernel density estimation of *QKI* expression for all T-ALL patients, we defined patients with normalized counts < 800 as the *QKI*-low group and the remaining as *QKI*-high (Figure 5B). Differential splicing analysis identified additional splicing events exclusively in the primary samples that were not observed in the T-ALL cell lines, underscoring the importance of analyzing both primary samples and cell lines. Noteworthy, of the 34 splicing changes detected in T-ALL cell lines, we validated 22 in the Verboom cohort (Figure 5C) and 23 in the TARGET T-ALL cohort (Figure 5D). Next, we examined the splicing patterns of *LRRFIP2* and *TCF12* in T-ALL patients with low and high *QKI* expression and compared them to those typically observed in healthy thymocytes. These two genes were selected as examples because their splicing was consistently altered in both T-ALL cell lines and primary T-ALL samples based on *QKI* expression levels. In both cohorts of T-ALL patients, the levels of *LRRFIP2* exon inclusion were comparable between those with high *QKI* expression and thymocytes. In contrast, patients with low *QKI* expression exhibited *LRRFIP2* exon skipping (Online Supplementary Figure S4A). Low-*QKI* T-ALL patients exhibited significantly higher inclusion of the *TCF12* ankyrin exon compared to high-*QKI* patients. Notably, this exon is rarely included in *TCF12* transcripts from healthy thymocytes, suggesting its inclusion in T-ALL is an aberrant splicing event resulting from reduced *QKI* expression (Online Supplementary Figure S4B).

Considering that T-ALL patients exhibit a wide range of *QKI* expression, we decided to determine whether there is an association between *QKI* expression and the corresponding ψ values of the perturbed splicing events. Linear regression analysis showed a strong positive correlation between *QKI* expression and ψ values (inclusion level) for events that are activated by *QKI* (Figure 6A) and a strong negative correlation for events that are repressed (Figure 6B).

Together, the data from T-ALL cell lines and primary patient samples indicate that *QKI* dysregulation is associated with

widespread splicing alterations in T-ALL, and the extent of these splicing changes closely correlate with *QKI* expression levels.

***QKI* negatively regulates T-cell acute lymphoblastic leukemia cell proliferation**

Reduced *QKI* expression in primary samples suggests a putative tumor-suppressive role of *QKI* in T-ALL. To investigate this hypothesis, we assessed the impact of ectopic *QKI* overexpression *in vitro* using the T-ALL cell line PF-382 and KARPAS-45. T-ALL cells were transduced with either a control construct or a *QKI* expression construct. Quantitative polymerase chain reaction (qPCR) analysis confirmed robust *QKI* overexpression in cells transduced with the *QKI* construct, showing approximately 20-fold and 25-fold increase in *QKI* mRNA levels in PF-382 and KARPAS-45 cells, respectively, compared with the control vector (Figure 7A, top). A concomitant increase in *QKI*-5 protein levels was verified by western blot analysis (Figure 7A, bottom). A proliferation assay demonstrated that PF-382 and KARPAS-45 cells expressing higher levels of *QKI* exhibited reduced proliferation compared to control cells (Figure 7B). To further validate the growth-suppressive function of *QKI*, we performed *QKI* knockdown in KOPT-K1 T-ALL cells using two independent shRNA targeting *QKI* (Figure 7C). Silencing *QKI* resulted in a significant increase in T-ALL cell proliferation compared to control cells, suggesting that *QKI* negatively regulates leukemic cell growth (Figure 7D). Consistent with these findings, *QKI*-depleted HPB-ALL cells (sh*QKI*) also resulted in increased cell growth compared with non-targeting control cells (shNTC) (Figure 7E). To elucidate the mechanism behind this growth difference, we examined both apoptosis and cell cycle progression. While no significant difference in apoptosis levels was detected upon either *QKI* overexpression or *QKI* silencing (Online Supplementary Figure S5A, C, E), we observed an arrest at G0/G1 transition in *QKI*-expressing T-ALL cells (Figure 7F, Online Supplementary Figure S5A, D). Conversely, *QKI* silencing in KOPT-K1 cells led to a decrease in the G0/G1 population and a corresponding increase in the G2/M fraction (Figure 7G, Online Supplementary Figure S5F), consistent with enhanced cell cycle progression.

Collectively, these findings demonstrate that *QKI* restrains T-ALL cell proliferation by modulating cell cycle dynamics, supporting its role as a negative regulator of leukemic cell proliferation.

***QKI* inhibits leukemia progression**

Next, we evaluated whether *QKI* overexpression affects T-ALL engraftment and disease progression *in vivo*, using human-to-mouse xenograft models. PF-382 and KARPAS-45 cells harboring either the control or *QKI* overexpression construct were transplanted into immunocompromised mice, and survival was monitored over time. Mice transplanted with cells over-expressing *QKI* had a significantly longer

median survival than control animals (PF-382; 42 days in *QKI*-OE compared to 22 days in control mice; KARPAS-45; 63 days in *QKI*-OE compared to 35 days in control mice, $P < 0.0001$) (Figure 8A, B), highlighting the impact of *QKI* on disease progression. Further analysis of leukemia burden, quantified by both the number and percentage of human CD45⁺ cells, revealed that mice with cells over-expressing *QKI* had significantly reduced infiltration of leukemic cells in the bone marrow, meninges, blood, testes, liver, spleen, and lungs (Figure 8C, D and *Online Supplementary Figure S6A, B*).

Collectively, these results indicate that *QKI* functions as a negative regulator of T-ALL progression, slowing disease progression and limiting leukemia burden across multiple organs.

Discussion

This study identifies the tumor-suppressive properties of *QKI* in leukemia, contributing to disease pathogenesis through its regulation of mRNA splicing. *QKI* dysregulation appears to be a distinctive feature of T-ALL, as evidenced by its markedly lower expression levels, particularly within the *HOXA* subgroup, across two independent pediatric T-ALL cohorts, compared to healthy thymocytes. This is in line with previous studies showing an inverse relationship between *QKI* expression and elevated *HOXA* gene levels in cases with *KMTA2* rearrangements, *CALM-AF10*, and *SET-NUP214* translocations,^{12,13,15} suggesting that *QKI* may play a subtype-specific role in T-ALL. Moreover, the stable expression of *QKI* across all stages of normal T-cell development further underscores that its reduced expression in T-ALL is likely an acquired feature related to malignancy rather than a reflection of typical developmental variation. Recent findings showed that reduced *QKI* expression leads to circRNA dysregulation in T-ALL.¹⁶ Together, these studies emphasize the significance of *QKI* dysregulation in driving RNA-level changes critical for T-ALL pathogenesis. The low *QKI* expression in T-ALL is significantly associated with poorer overall survival, supporting the view that *QKI* is a potential marker and offering a therapeutic window to restore alternative splicing patterns disrupted by reduced *QKI* levels.

Notably, mutations or copy number losses affecting *QKI* are infrequent; they are observed in only a minority of patients in the TARGET cohort, pointing instead to epigenetic mechanisms as the primary drivers of *QKI* dysregulation. Consistent with this, we observed *QKI* promoter hypermethylation in the LOUCY and KARPAS-45 T-ALL cell lines, both of which exhibit minimal *QKI* expression. We and others have shown that this epigenetic regulation shapes leukemic transcriptional programs.⁴¹ This pattern of DNA methylation-driven silencing mirrors that of other tumor suppressors, such as *TET2*,³⁷ which clustered with *QKI* in

gene expression analyses (*Online Supplementary Figure S1F*) and is similarly subject to hypermethylation in T-ALL. The preferential reduction of *QKI* in *HOXA*-positive T-ALL, together with promoter hypermethylation in the *HOXA*-driven LOUCY cell line, suggests that *HOXA*-associated epigenetic programs may contribute to *QKI* silencing. Although we cannot definitively conclude that *HOXA* directly silences *QKI*, our data suggest that *QKI* downregulation in T-ALL is mediated by epigenetic modifications rather than direct genetic alterations, adding *QKI* to the growing list of epigenetically-regulated tumor suppressors in T-ALL.

Functional studies in cell lines and mouse models provided additional evidence that *QKI* contributes to T-ALL progression by promoting aberrant splicing and altering gene expression profiles. Furthermore, knockdown experiments in T-ALL cell lines, combined with transcriptome analyses, showed that *QKI* depletion induces significant splicing changes, especially in cassette exons, affecting genes involved in key cellular pathways such as Wnt/ β -catenin signaling and EMT. Notably, we observed increased exon skipping in *LRRFIP2*, *CIT*, and *AKAP9*, along with enhanced exon inclusion in *CD47*, *ESYT2*, and *TCF12*, indicating that, as in solid tumors,^{23,24} *QKI* plays both repressive and activating roles in modulating splicing patterns in T-ALL. This is in line with previous reports that *QKI* displays position-dependent regulation, promoting inclusion when bound to a downstream intronic splicing enhancer (ISE) and repressing exon inclusion when bound to an upstream exonic splicing silencer (ESS).^{26,29} Importantly, these splicing changes were validated in both T-ALL cell lines and two independent T-ALL patient cohorts, highlighting the consistency of these findings across multiple models. *LRRFIP2* and *TCF12* emerged as key examples, exhibiting exon inclusion or skipping in a manner that strongly correlated with *QKI* expression levels in primary samples. While some of the *QKI*-regulated splicing changes were identified previously in solid tumors, such as *ADD3* and *CD47*, others, like *TCF12* and *ERBIN*, appear unique to T-ALL. This distinct splicing profile supports the notion that the role of *QKI* in T-ALL is influenced by the specific cellular context, potentially due to interactions with other splicing regulators that vary across tissues.

TCF12 (*HEB*) is essential for normal T-cell development.^{42,43} It can produce two main isoforms, a longer canonical isoform (HEBCan) and a shorter alternative isoform (HEBAlt), due to two distinct transcription start sites.⁴⁴ While HEBCan is expressed across all stages of T-cell development, HEBAlt is confined to the double-negative stages (CD4⁻CD8⁻). *QKI* depletion led to the inclusion of a 72 bp exon encoding an ankyrin-like repeat. Although this ankyrin-like exon can be incorporated into HEBCan, it was previously excluded in studies as it does not appear in transcripts from thymocyte cDNA libraries,⁴⁵ suggesting it may be specifically associated with T-ALL rather than normal T-cell development. While the functional consequences of this insertion

have not been extensively explored, prior research in the rat homolog (REB) showed that this insertion significantly diminished the ability of REB to bind specific E-box-binding sites and to form both homodimers and heterodimers with other bHLH family members.⁴⁶

Reduced *QKI* expression in T-ALL leads to *LRRFIP2* exon 7 skipping. In gastric cancer, the isoform switching of *LRRFIP2* is regulated by the epithelial splicing regulatory protein (*ESRP1*), an epithelial-specific RNA-binding protein involved in the alternative splicing of EMT-related genes, which are critical for metastasis. The mesenchymal isoform of *LRRFIP2* includes exon 7, promoting metastatic potential, whereas exon 7 skipping has been linked to metastasis suppression.⁴⁷ Thus, *ESRP1* acts as a negative regulator of *LRRFIP2* exon 7, while *QKI* functions as a positive splicing factor. *ESRP1* was also found to regulate the alternative splicing of *CD47*, an event which is similarly modulated by *QKI* in T-ALL. Interestingly, *ESRP1* is hardly expressed at all in T-ALL (*data not shown*), suggesting that while *ESRP1* and *QKI* may share common splicing targets, they likely play tissue-specific roles.

The enrichment of EMT-associated pathways among the *QKI*-regulated splicing events and the gene expression profiles observed following *QKI* knockdown provides further insight into T-ALL biology. EMT-like changes are increasingly recognized in hematologic malignancies, where they are thought to promote cellular plasticity, invasiveness, and treatment resistance.⁴⁸ Our findings indicate that *QKI* dysregulation may induce EMT-like properties in T-ALL, potentially facilitating leukemic cell dissemination and infiltration. This aligns with reports in solid tumors where *QKI* has been shown to regulate EMT-related splicing,^{23,24} highlighting the conserved nature of its function across cancer types and further implicating EMT as an important mechanism in T-ALL progression.

At the transcriptomic level, *QKI* silencing led to the differential expression of hundreds of genes, impacting pathways related to cell cycle, mitosis, and the G2M checkpoint. Notably, marginal overlap between genes affected by differential expression and those with splicing alterations suggests that *QKI* may have but an indirect impact on gene expression, an impact which is mediated through its splicing function rather than direct transcriptional regulation. This separation of splicing and transcriptional functions reinforces the role of *QKI* as a crucial modulator of post-transcriptional regulation in T-ALL.

Our functional studies support the tumor-suppressive properties of *QKI* in T-ALL. Forced expression of *QKI* in T-ALL cell lines led to a marked reduction in cell proliferation, accompanied by G0/G1 cell cycle arrest, without significantly affecting apoptosis. Consistent with this observation, previous studies have shown that *QKI*-5 overexpression inhibits cell proliferation and induces G0/G1 arrest in non-small cell lung cancer (NSCLC) and clear cell renal cell carcinoma (ccRCC) cell lines.^{49,50} These results underscore

the conserved role of *QKI* in regulating the cell cycle across different cancer types. Collectively, these findings suggest that *QKI* inhibits leukemic growth by regulating the cell cycle rather than promoting cell death. Furthermore, *in vivo* xenograft experiments provided compelling evidence of the tumor-suppressive role of *QKI* in T-ALL, with *QKI* overexpression significantly reducing leukemia burden and extending survival in mice.

Integrating all obtained data enabled us to define the specific substrate pool of *QKI*-driven splicing events. Given the pervasive role of *QKI* in T-ALL, therapeutic strategies aimed at compensating for its function loss or mitigating its downstream effects could benefit patients, particularly those within the HOXA subgroup. Potential approaches might include reversing the epigenetic silencing to partially restore *QKI* activity or, alternatively, targeting downstream pathways and specific splicing events that become dysregulated in the absence of sufficient *QKI* levels. Given the absence of *QKI* CLIP-seq or eRIC datasets and the technical difficulties of generating high-quality CLIP data for *QKI*, our study cannot directly showcase direct *QKI* causality to the splicing changes observed. Alternative approaches (e.g., eCLIP, TRIBE-seq) may help define direct *QKI* targets. Future studies are required to investigate the upstream factors and epigenetic regulators responsible for *QKI* downregulation in T-ALL, along with a deeper characterization of the isoforms and molecular mechanisms impacted by the resulting alternative splicing events.

Disclosures

No conflicts of interest to disclose.

Contributions

BP is responsible for study concept, formal analysis, data curation, visualization, investigation, methodology, and writing the original draft. NDS is responsible for investigation, formal analysis, and writing, reviewing and editing the manuscript. IF and TP are responsible for data interpretation, and writing, reviewing and editing the manuscript. DD and FVN are responsible for resources, methodology and investigation. PM is responsible for study design and supervision, and data interpretation. PN is responsible for funding acquisition, study concept, design and supervision, data interpretation, project administration, and writing, reviewing and editing the manuscript. KM-W is responsible for funding acquisition, study concept, design and supervision, data interpretation, and writing, reviewing and editing the manuscript. PVV was responsible for funding acquisition, study concept, design and supervision, data interpretation, and project administration.

Acknowledgments

We thank Sara Dufour from the VIB Proteomics Core (PRC) for her valuable assistance with the analysis of the proteomics data.

Funding

This study is supported by the Baillet Latour Grant for Medical research 2018 granted (to PVV) and the Bilateral research cooperation China (FWO) (grant number G0E6222N). The Matlawska lab is supported by grants from the National Cancer Institute (NCI) at the National Institutes of Health (NIH) (grant numbers R01 CA237165, R01 CA282701). The Ntziachristos laboratory is supported by the Research Foundation Flanders (FWO) (grant numbers G0F4721N, G0A8B24N); start-up funds from the Department of Biomolecular Medicine, Ghent University, a Flanders interuniversity consortium grant (grant number BOF.IBO.2023.0006.02); and a Cancer Research Institute Ghent (CRIG) partnership grant.

Data-sharing statement

All raw RNA-Seq data generated in this study have been deposited in the NCBI Gene Expression Omnibus (GEO, <https://www.ncbi.nlm.nih.gov/geo/>) under accession number GSE281561. The proteomics data have been deposited in the PRIDE repository (<https://www.ebi.ac.uk/pride/>) and are accessible under accession number PXD058761. RNA-

Seq data for T-ALL cell lines from Leo et al.³⁵ were retrieved from Sequence Read Archive (SRA) under accession number PRJNA707100, while RNA-Seq data from CCLE³⁶ were accessed via SRA under accession number PRJNA523380. To facilitate comparison between cell lines, only those with at least two replicates were included in the analysis. The RNA-seq data for primary T-ALL samples analyzed in this study are publicly available through the Database of Genotypes and Phenotypes (dbGaP) under the parent accession number phs000218 and its substudy accession number phs000464 (TARGET: Acute Lymphoblastic Leukemia (ALL) Expansion Phase 2)³ and the Sequence Read Archive (SRA) under accession number PRJNA434176 (Verboom cohort).³² Additionally, RNA-seq data for 24 healthy thymocyte samples reported by Sun et al.³² were retrieved from the SRA under accession number PRJNA741323. All datasets, encompassing both primary T-ALL samples and healthy thymocytes, were integrated and normalized using the DESeq2 package in R. The methylation data from T-ALL cell lines were obtained from GEO under accession number GSE68379 (Infinium HumanMethylation 450 BeadChip) and PRJNA523380 (CCLE).

References

- Iacobucci I, Mullighan CG. Genetic basis of acute lymphoblastic leukemia. *J Clin Oncol*. 2017;35(9):975-983.
- Hunger SP, Mullighan CG. Acute lymphoblastic leukemia in children. *N Engl J Med*. 2015;373(16):1541-1552.
- Liu Y, Easton J, Shao Y, et al. The genomic landscape of pediatric and young adult T-lineage acute lymphoblastic leukemia. *Nat Genet*. 2017;49(8):1211-1218.
- Brady SW, Roberts KG, Gu Z, et al. The genomic landscape of pediatric acute lymphoblastic leukemia. *Nat Genet*. 2022;54(9):1376-1389.
- Marks DI, Rowntree C. Management of adults with T-cell lymphoblastic leukemia. *Blood*. 2017;129(9):1134-1142.
- Teachey DT, O'Connor D. How I treat newly diagnosed T-cell acute lymphoblastic leukemia and T-cell lymphoblastic lymphoma in children. *Blood*. 2020;135(3):159-166.
- Chen S, Benbarche S, Abdel-Wahab O. Splicing factor mutations in hematologic malignancies. *Blood*. 2021;138(8):599-612.
- Black KL, Naqvi AS, Asnani M, et al. Aberrant splicing in B-cell acute lymphoblastic leukemia. *Nucleic Acids Res*. 2018;46(21):11357.
- Zhou Y, Han C, Wang E, et al. Posttranslational regulation of the exon skipping machinery controls aberrant splicing in leukemia. *Cancer Discov*. 2020;10(9):1388-1409.
- Han C, Khodadadi-Jamayran A, Lorch AH, et al. SF3B1 homeostasis is critical for survival and therapeutic response in T cell leukemia. *Sci Adv*. 2022;8(3):eabj8357.
- Neumann DP, Goodall GJ, Gregory PA, Philip Gregory CA. The Quaking RNA-binding proteins as regulators of cell differentiation. *Wiley Interdiscip Rev RNA*. 2022;13(6):e1724.
- Van Vlierberghe P, van Grotel M, Tchinda J, et al. The recurrent SET-NUP214 fusion as a new HOXA activation mechanism in pediatric T-cell acute lymphoblastic leukemia. *Blood*. 2008;111(9):4668-4680.
- Dik WA, Brahim W, Braun C, et al. CALM-AF10+ T-ALL expression profiles are characterized by overexpression of HOXA and BMI1 oncogenes. *Leukemia*. 2005;19(11):1948-1957.
- Ferrando AA, Armstrong SA, Neuberg DS, et al. Gene expression signatures in MLL-rearranged T-lineage and B-precursor acute leukemias: dominance of HOX dysregulation. *Blood*. 2003;102(1):262-268.
- Kang H, Sharma ND, Nickl CK, et al. Dysregulated transcriptional networks in KMT2A- and MLLT10-rearranged T-ALL. *Biomark Res*. 2018;6(1):27.
- Buratin A, Palhais B, Gaffo E, et al. Depletion of the RNA binding protein QKI and circular RNA dysregulation in T-cell acute lymphoblastic leukemia. *Haematologica*. 2025;110(4):972-979.
- Ebersole TA, Chen Q, Justice MJ, Artzt K. The quaking gene product necessary in embryogenesis and myelination combines features of RNA binding and signal transduction proteins. *Nat Genet*. 1996;12(3):260-265.
- Wu J, Zhou L, Tonissen K, Tee R, Artzt K. The Quaking I-5 protein (QKI-5) has a novel nuclear localization signal and shuttles between the nucleus and the cytoplasm. *J Biol Chem*. 1999;274(41):29202-29210.
- Wu JI, Reed RB, Grabowski PJ, Artzt K. Function of quaking in myelination: regulation of alternative splicing. *Proc Natl Acad Sci*. 2002;99(7):4233-4238.
- Galarneau A, Richard S. Target RNA motif and target mRNAs of the Quaking STAR protein. *Nat Struct Mol Biol*. 2005;12(8):691-698.
- Bockbrader K, Feng Y. Essential function, sophisticated regulation and pathological impact of the selective RNA-binding protein QKI in CNS myelin development. *Future Neurol*. 2008;3(6):655-668.
- Zong FY, Fu X, Wei WJ, et al. The RNA-binding protein QKI suppresses cancer-associated aberrant splicing. *Cheung VG, ed. PLoS Genet*. 2014;10(4):e1004289.
- Pillman KA, Phillips CA, Roslan S, et al. miR-200/375 control

- epithelial plasticity-associated alternative splicing by repressing the RNA-binding protein Quaking. *EMBO J.* 2018;37(13):e99016.
24. Li J, Choi PS, Chaffer CL, et al. An alternative splicing switch in *FLNB* promotes the mesenchymal cell state in human breast cancer. *Elife.* 2018;7:e37184.
 25. Chen X, Yin J, Cao D, et al. The emerging roles of the RNA binding protein *QKI* in cardiovascular development and function. *Front Cell Dev Biol.* 2021;9:668659.
 26. Wang JZ, Fu X, Fang Z, et al. *QKI-5* regulates the alternative splicing of cytoskeletal gene *ADD3* in lung cancer. *J Mol Cell Biol.* 2021;13(5):347-360.
 27. Montañés-Agudo P, Aufiero S, Schepers EN, et al. The RNA-binding protein *QKI* governs a muscle-specific alternative splicing program that shapes the contractile function of cardiomyocytes. *Cardiovasc Res.* 2023;119(5):1161-1174.
 28. Liberzon A, Birger C, Thorvaldsdóttir H, Ghandi M, Mesirov JP, Tamayo P. The molecular signatures database (MSigDB) hallmark gene set collection. *Cell Syst.* 2015;1(6):417-425.
 29. Vaquero-Garcia J, Aicher JK, Jewell S, et al. RNA splicing analysis using heterogeneous and large RNA-seq datasets. *Nat Commun.* 2023;14(1):1230.
 30. Kesel JD, Fijalkowski I, Taylor J, Ntziachristos P. Splicing dysregulation in human hematologic malignancies: beyond splicing mutations. *Trends Immunol.* 2022;43(8):674-686.
 31. Verboom K, Van Loocke W, Volders PJ, et al. A comprehensive inventory of *TLX1* controlled long non-coding RNAs in T-cell acute lymphoblastic leukemia through polyA+ and total RNA sequencing. *Haematologica.* 2018;103(12):e585-e589.
 32. Sun V, Sharpley M, Kaczor-Urbanowicz KE, et al. The metabolic landscape of thymic T cell development in vivo and in vitro. *Front Immunol.* 2021;12:716661.
 33. Pölönen P, Di Giacomo D, Seffernick AE, et al. The genomic basis of childhood T-lineage acute lymphoblastic leukaemia. *Nature.* 2024;632(8027):1082-1091.
 34. Leo IR, Aswad L, Stahl M, et al. Integrative multi-omics and drug response profiling of childhood acute lymphoblastic leukemia cell lines. *Nat Commun.* 2022;13(1):1691.
 35. Ghandi M, Huang FW, Jané-Valbuena J, et al. Next-generation characterization of the Cancer Cell Line Encyclopedia. *Nature.* 2019;569(7757):503-508.
 36. Roels J, Thénoz M, Szarzyńska B, et al. Aging of preleukemic thymocytes drives CpG island hypermethylation in T-cell acute lymphoblastic leukemia. *Blood Cancer Discov.* 2020;1(3):274-289.
 37. Bensberg M, Rundquist O, Selimovic A, et al. *TET2* as a tumor suppressor and therapeutic target in T-cell acute lymphoblastic leukemia. *Proc Natl Acad Sci U S A.* 2021;118(34):e2110758118.
 38. De Coninck S, Roels J, Lintermans B, et al. *Tet2* is a tumor suppressor in the preleukemic phase of T-cell acute lymphoblastic leukemia. *Blood Adv.* 2024;8(11):2646-2649.
 39. Iorio F, Knijnenburg TA, Vis DJ, et al. A landscape of pharmacogenomic interactions in cancer. *Cell.* 2016;166(3):740-754.
 40. Subramanian A, Tamayo P, Mootha VK, et al. Gene set enrichment analysis: a knowledge-based approach for interpreting genome-wide expression profiles. *Proc Natl Acad Sci.* 2005;102(43):15545-15550.
 41. Fang C, Wang Z, Han C, et al. Cancer-specific CTCF binding facilitates oncogenic transcriptional dysregulation. *Genome Biol.* 2020;21(1):247.
 42. Yoganathan K, Yan A, Rocha J, et al. Regulation of the signal-dependent E protein *HEBAIt* through a *YYY* motif is required for progression through T cell development. *Front Immunol.* 2022;13:848577.
 43. Braunstein M, Anderson MK. Developmental progression of fetal *HEB-/-* precursors to the pre-T-cell stage is restored by *HEBAIt*. *Eur J Immunol.* 2010;40(11):3173-3182.
 44. Kee BL. *E* and *ID* proteins branch out. *Nat Rev Immunol.* 2009;9(3):175-184.
 45. Wang D, Claus CL, Vaccarelli G, et al. The basic helix-loop-helix transcription factor *HEBAIt* is expressed in pro-T cells and enhances the generation of T cell precursors. *J Immunol.* 2006;177(1):109-119.
 46. Klein ES, Simmons DM, Swanson LW, Rosenfeld MG. Tissue-specific RNA splicing generates an ankyrin-like domain that affects the dimerization and DNA-binding properties of a bHLH protein. *Genes Dev.* 1993;7(1):55-71.
 47. Lee J, Pang K, Kim J, et al. *ESRP1*-regulated isoform switching of *LRRFIP2* determines metastasis of gastric cancer. *Nat Commun.* 2022;13(1):6274.
 48. Varisli L, Vlahopoulos S. Epithelial-mesenchymal transition in acute leukemias. *Int J Mol Sci.* 2024;25(4):2173.
 49. Zhu W, Yu Y, Fang K, et al. *miR-31/QKI-5* axis facilitates cell cycle progression of non-small-cell lung cancer cells by interacting and regulating *p21* and *CDK4/6* expressions. *Cancer Med.* 2023;12(4):4590-4604.
 50. Zhang RL, Yang JP, Peng LX, et al. RNA-binding protein *QKI-5* inhibits the proliferation of clear cell renal cell carcinoma via post-transcriptional stabilization of *RASA1* mRNA. *Cell Cycle.* 2016;15(22):3094-3104.